



HAL
open science

Fractional dynamics in silk: From molecular picosecond subdiffusion to macroscopic long-time relaxation

Igor Krasnov, Tilo Seydel, Martin Müller

► To cite this version:

Igor Krasnov, Tilo Seydel, Martin Müller. Fractional dynamics in silk: From molecular picosecond subdiffusion to macroscopic long-time relaxation. *Physical Review E : Statistical, Nonlinear, and Soft Matter Physics* [2001-2015], 2015, 91 (4), <10.1103/PhysRevE.91.042716>. <hal-03117119>

HAL Id: hal-03117119

<https://hal.science/hal-03117119v1>

Submitted on 20 Jan 2021

HAL is a multi-disciplinary open access archive for the deposit and dissemination of scientific research documents, whether they are published or not. The documents may come from teaching and research institutions in France or abroad, or from public or private research centers.

L'archive ouverte pluridisciplinaire **HAL**, est destinée au dépôt et à la diffusion de documents scientifiques de niveau recherche, publiés ou non, émanant des établissements d'enseignement et de recherche français ou étrangers, des laboratoires publics ou privés.



HAL Authorization

Fractional dynamics in silk: From molecular picosecond subdiffusion to macroscopic long-time relaxation

Igor Krasnov,^{1,2} Tilo Seydel*,³ and Martin Müller²

¹*Institut für Experimentelle und Angewandte Physik, Universität Kiel, D-24098 Kiel, Germany*

²*Institute of Materials Research, Helmholtz-Zentrum Geesthacht (HZG), D-21502 Geesthacht, Germany*

³*Institut Max von Laue – Paul Langevin (ILL), CS 20156, F-38042 Grenoble, France*

(Dated: April 28, 2015)

Structural relaxations in humid silk fibers exposed to tensile stress have been reported to take place on a very wide range of time scales from a few milliseconds to several hours. The time-dependence of the measured tensile force following a quasi-instantaneously applied external strain on the fibers can be understood in terms of a fractional viscoelastic relaxation function introducing memory effects by which the mechanical state of a fiber depends on its tensile history. An analog fractional relaxation also gives rise to the subdiffusion observed on picosecond time scales which governs the mobility of the amorphous polymer chains and adsorbed water on the molecular level. The reduction of the subdiffusive memory effect in stretched fibers compared to native fibers is consistent with the higher order of the polymers in the stretched state.

PACS numbers: 62.20.F-, 87.14.em, 87.15.H-, 87.15.La, 87.64.Bx, 02.50.Ey

Silk fibers from spiders and silkworms are known for their extraordinarily high toughness defined as the integral over the stress-strain curve [1, 2]. An underlying hierarchical nanocomposite polymer arrangement gives rise to this toughness. In particular, the combination of nanocrystallite, amorphous, and smectic regions [3, 4] within the polymer material is assumed to contribute most significantly to the mechanical properties. Silk fibers from various invertebrate, and notably from spiders and silkworms, are morphologically similar [5, 6] and based on similar proteins, with spider silk fibers being the mechanically most advanced fibers. Silk fibers appear to undergo a continuous rearrangement when exposed to an externally applied constant mechanical strain [7]. This assumed molecular rearrangement is macroscopically reflected by a continuously decreasing tensile force [8, 9]. The decrease of the tensile force sets on immediately following the application of the external strain and continues with an asymptotically decaying effect on a time scale of several days. Water adsorbed by the silk fibers drastically alters the mechanical properties by giving them an increasingly rubber-like habitus [10] and seems to even enhance the long-time structural rearrangements. Importantly, it has been confirmed that water only accesses the amorphous fraction of the silk fibers [4, 11], where it contributes to a breakup of the hydrogen bonds and a subsequent plasticization of the polymer chains. The mechanical properties of silk fibers appear to be consistent with a model of entropy elasticity known also for rubber [10], where the increasing order of the amorphous polymer chains constitutes the restoring force opposing the external tensile force.

It is of high interest to explore the changes occurring in the silk fibers on molecular length and time scales and to establish a link with the changes observable on macroscopic observation scales. In recent years, the viscoelastic mechanical properties of various polymer materials have been successfully described based on fractional relaxation relations [12–14] inspired by the more general theory of memory effects by Zwanzig [15]. This motivates the idea to also apply a fractional model to the underlying molecular processes. In this paper, we analyze both the macroscopically observed mechanical relaxation of humid silk fibers as well as the Brownian diffusion occurring on a level of molecular dynamics within the silk’s water-plasticized polymer chains using the fractional model. We experimentally access the molecular motion on nanometer length scales and picosecond time scales using incoherent quasi-elastic neutron spectroscopy probing the dynamic self-correlation function of the prevailing hydrogen atoms in silk fibers, and we test the effect of a tensile force by applying it *in situ* during the neutron scattering experiment. The difficulty in this approach arises from the fact that the neutron scattering experiment requires an integration time of a few hours during which the silk fibers undergo the above-mentioned slow structural rearrangement. Nevertheless, the fractional dynamics model incorporates this fact.

Similar to the ‘classical’ viscoelastic and diffusion phenomena, the description of the anomalous sub-diffusion and fractional viscoelasticity is based on a relaxation equation, but with derivatives of non-integer order [16–18]. The latter can be formulated in terms of the fractional calculus as [16]:

$${}^C D^\alpha [\Phi](t) = -\frac{1}{\tau^\alpha} \Phi(t). \quad (1)$$

Therein, ${}^C D^\alpha$ is the fractional derivative of Caputo type,

*e-mail: seydel@ill.eu

which for the case $0 \leq \alpha \leq 1$ can be defined as

$${}_0^C D^\alpha [\Phi](t) = \frac{1}{\Gamma(1-\alpha)} \int_0^t \frac{\Phi'(\xi)}{(t-\xi)^\alpha} d\xi \quad (2)$$

where $\Phi'(\xi)$ denotes the first order derivative of the function $\Phi(\xi)$. The solution of Eq. (1) is given by the Mittag-Leffler function $E_{\alpha,1}(-|t/\tau|^\alpha)$, generally defined as

$$E_{\alpha,\beta}(z) = \sum_{n=0}^{\infty} \frac{z^n}{\Gamma(\alpha n + \beta)}. \quad (3)$$

For $\alpha \rightarrow 1$ Eq. (1) becomes the usual (Debye) relaxation with the exponential function as its solution. However, for $\alpha \neq 1$ this equation becomes a non-local integro-differential equation with a solution that interpolates between a (stretched) exponential law for small t and an inverse power law for large t . The solution of this equation (or its inhomogeneous version) appears in all fractional viscoelastic models, where it governs the behavior of the so-called fractional dash-pot viscoelastic element.

Single-fiber mechanical test experiments (Fig. 1, symbols) were performed using the sample cell previously described in Ref. [9] consisting of a piezo-electric actuator and highly sensitive force sensor embedded in a humidity chamber at ambient temperature. The fit function describing the fractional viscoelastic response based on Eq. (1), also denoted generalized Zener model of fractional viscoelasticity [14], (solid line in Fig. 1) was evaluated using block-pulse functions [19]. The resulting fit parameter is $\alpha = 0.62 \pm 0.03$ ($\tau = 1.11$ s). The fit using the fractional model describes the stress relaxation extremely well over several orders of magnitude in the observation time with only few parameters. By contrast, the ‘classical’ exponential decay and inverse power laws (dashed lines in Fig. 1) can only model the short-time and long-time limits of the relaxation, respectively. It is remarkable that the fractional relaxation equation is closely connected to anomalous (continuous) random walks (of e.g. trapping or constrained type) [17]. This leads to the identification of the parameter α in Eq. (1) with the Lévy index of the waiting time distribution function of the hopping process (see e.g. [16]). The models of the trapped random walks are frequently used to describe glassy or dynamically frustrated systems [16]. Hence the viscoelastic models based on Eq. (1) are related to the stochastic behavior on a more microscopic (molecular) level.

To access the dynamics of silk at the molecular level, *in situ* neutron scattering experiments were performed using the time-of-flight spectrometer IN6 at the ILL with an incident wavelength of 5.1 \AA . Neutron spectroscopy requires a bundle of silk to be illuminated by the beam to obtain the required scattering volume. An uninterrupted fiber of degummed *Bombyx mori* silkworm silk was wound repeatedly (11847 turns [20]) around a pair

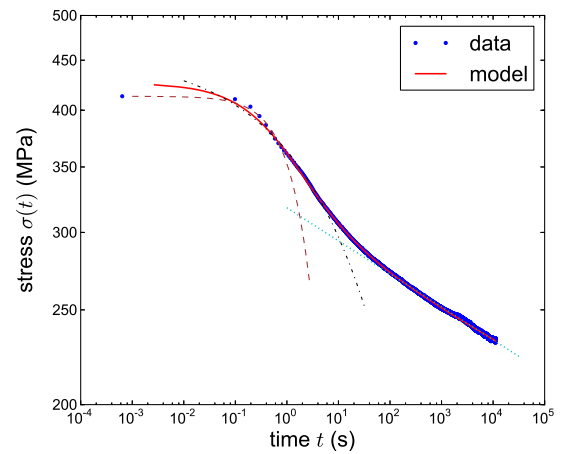


FIG. 1: (Color online) Mechanical relaxation of a single *Bombyx mori* silk fiber (symbols). The cyan dotted line depicts the inverse power $t^{-\alpha}$ and the brown dashed line the exponential decay law, while the black dash-dotted line shows the stretched exponential $\exp(-|t/\tau|^\beta)$. The fractional relaxation function (solid line) interpolates between these decay laws.

of steel hooks attached to a tensile apparatus and surrounded by a hermetically sealed chamber containing air saturated with H_2O . This setup was inserted into the sample bay of IN6 such that the neutron scattering plane was perpendicular to the fiber axis. The total fiber mass prior to humidification amounted to 190.6 ± 0.1 mg [20]. The measured data were reported previously in Ref. [20]. The model-free analysis of the elastic incoherent structure factor (EISF) [20] yields a typical length scale of 1 nm for the observed picosecond dynamics. The part of the spectra associated with quasi-elastic scattering (QENS) – i.e. diffusive motions – was previously analyzed in terms of a superposition of constrained and unconstrained jumps and constrained continuous diffusion [20]. The previous model describes the QENS data only in a subregion of the accessible range of energies and momentum transfers and is rather of a qualitative character. Nevertheless, the earlier analysis already provides strong evidence for the presence of sub-diffusional dynamics.

Incoherent neutron spectroscopy accesses both temporal and spatial single-particle atomic self-correlations via the van Hove autocorrelation function $W(r, t)$. The measured intensity is closely related to the scattering function $S(Q, \omega)$ and the intermediate scattering function $I(Q, t)$; both are obtained by Fourier transform from $W(r, t)$. Here r denotes the spatial distance, Q the momentum transfer, t the time, and ω the frequency. The fractional diffusion model [17], sometimes denoted a fractional random walk, is used to model the internal molecular dynamics of humid silk as seen through $W(r, t)$. In this model the correlation function obeys the generalized dif-

fusion equation:

$${}^C D^\alpha W(r, t) = K_\alpha \nabla^2 W(r, t) \quad (4)$$

where K_α is the generalized diffusion coefficient

$$K_\alpha = \frac{\sigma_c^2}{\tau_c^\alpha}. \quad (5)$$

Therein, σ_c and τ_c are characteristic spatial and time scales, respectively. The model requires only two parameters, α and K_α , to describe the behavior of the system. For $\alpha = 1$ we have classical Fickian diffusion, while $0 < \alpha < 1$ indicates fractional sub-diffusion. The spatially Fourier-transformed Eq. (4) is equivalent to Eq. (1) and, hence, it is solved by the Mittag-Leffler function, Eq. (3), resulting in the quasi-elastic component of the intermediate scattering function:

$$I(Q, t) \sim E_{\alpha, 1} \left(- \left| \frac{t}{\tau} \right|^\alpha \right) \quad \text{with} \quad \tau = (K_\alpha Q^2)^{-1/\alpha} \quad (6)$$

with the fractional relaxation time τ .

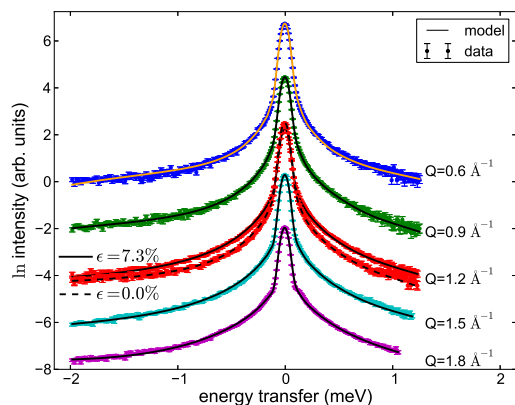


FIG. 2: (Color online) Neutron spectra recorded on humid (H_2O 100 % RH) *Bombyx silk* silk fibers (symbols) in a native (displayed only for $Q = 1.2 \text{ \AA}^{-1}$) and stretched (7.3 %) state, respectively, at ambient temperature. The fits with Eq. (6) have been carried out simultaneously for all Q .

Fig. 2 depicts the experimental results from neutron spectroscopy on humid (H_2O) silk fibers for different values of Q and different values of the externally applied elongation (symbols). All data have been reduced as reported previously [20]. In the numerical implementation of the fits (lines), the Fourier transform of $R(Q, t) \cdot I(Q, t)$ was fitted to the experimental data for $S(Q, \omega)$. Therein, $I(Q, t)$ denotes the model scattering function (Eq. 6) and $R(Q, t)$ the analytical description of the experimental resolution in the time domain obtained from a spline fit of the spectrum $R(Q, \omega)$ of dry silk [20] which was subsequently Fourier transformed using an FFT algorithm.

The fits have been carried out simultaneously for all Q . The Mittag-Leffler-function, Eq. (3), was computed using the algorithm by Hilfer and Seybold [21].

strain (%)	α	$K_\alpha \left(\frac{\text{\AA}^2}{\text{ps}^\alpha} \right)$
0	0.56 ± 0.02	0.0525 ± 0.0006
4.7	0.75 ± 0.02	0.12 ± 0.005
7.3	0.74 ± 0.02	0.12 ± 0.005

TABLE I: Fit results for the neutron spectra using the fractional diffusion model, Eq. (4). The errors denote the 95 % confidence limits obtained from the Jacobian of the variable-metric fit algorithm subsequent to convergence.

We observe that the fit using the fractional relaxation model describes our data very well and indeed better than the ‘classical’ fit published earlier [20]. The resulting fit parameters are summarized in table I. The values for α (table I) strongly deviating from unity indicate the presence of memory effects in the molecular diffusion in humid silk. We further observe that the diffusion law in the unstretched (native) fiber – being in an equilibrium state – is different from the stretched one, which undergoes a continuous mechanical relaxation (cf. Fig. 1). The increase of α with applied strain indicates a partial loss of the ‘memory’ in the system. Significantly further increasing the strain from 4.7 % to 7.3 % causes only a very small further variation in the parameters. This is consistent with a high similarity of the molecular diffusion processes on which the long-time relaxation is based. Furthermore, the value $\alpha = 0.62$ for the mechanical relaxation, lying between the corresponding fitted values for the molecular relaxation, is consistent with an interpolation from the highly stretched state of the fiber towards the native state [9] over the time of the experiment. Our neutron spectroscopy results are based on measurements over a relatively long integration time scale of several hours.

The observation from the fit with the fractional relaxation model is also in agreement with the trend observed using the earlier ‘classical’ fits [20]. The latter already suggest faster diffusion processes with increasing stress. Both the old and the new picture are consistent with the assumption that the water-plasticized humid silk fibers are further plasticized by the stress: The applied stress causes a loss of memory and a decrease of the relaxation time. We hypothesize that this stress-related plasticization effect is due to the increased exposure of the unraveled amorphous polymer chains to water molecules under tensile load.

The success of the model of fractional dynamics leads us to assume that the movement of single water molecules and peptide chains in humid silk occurs in a strongly correlated fashion: many transport processes are strongly interconnected and their mutual influence causes memory effects. We assume that it is this unifying collective character of the dynamics which allows us to describe the dissipative behavior of such a complex system by a model

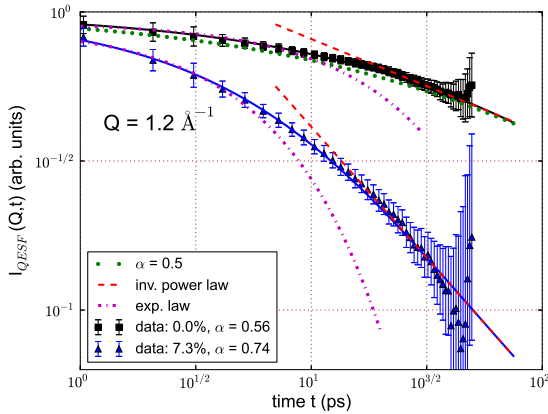


FIG. 3: (Color online) QENS component of the intermediate scattering function $I(Q, t)$ for two states of stretching at $Q = 1.2 \text{ \AA}^{-1}$. Squares represent measurements of the native ($\epsilon = 0\%$) and triangles of the stretched sample ($\epsilon = 7.3\%$), respectively. Solid lines represent the model function eq. (6) with parameters from table I. The fractional relaxation times corresponding to the momentum transfer shown are $\tau \approx 95$ ps for $\epsilon = 0\%$ and $\tau \approx 10$ ps for $\epsilon = 7.3\%$. The dotted line demonstrates the behavior of $I(Q, t)$ at $\alpha = 1/2$ (Rouse model [22, 23]). The dashed line denotes the inverse power and dash-dotted line the exponential relaxation, respectively.

with only a few parameters. In this context we emphasize that the unstretched fibers in our experiment were at no time pre-stretched prior to the experiment, but in their native state. The results concerning the long-time mechanical relaxation experiments and our fit of the QENS spectra by the fractional diffusion dynamics are qualitatively similar. Both show the presence of memory effects: one on the time scale of several hours/days and the other on the molecular time scales from picoseconds to nanoseconds. Generally, it appears that memory effects propagate from the molecular to the macroscopic level and find their manifestation also in the mechanical long-time relaxation phenomena. An explanation for the fundamental cause of this connection between the molecular and macroscopic scales via the memory effect may find inspiration in the self-similar ladder model [23]. The fractional diffusion model on a molecular scale is also promising for applications in other complex soft matter systems, including proteins in general [24], where motions take place over a wide range of time scales. Our new numerical approach introduces a significant innovation compared to earlier work in this direction by allowing for a free fit parameter α and a global fit for all Q . Compared to the discussion of polymer fibers in terms of models derived from Rouse's theory [22], corresponding to $\alpha = 1/2$ [23], our much more general fractional calculus allows to discriminate native from stretched fibers

via the inclusion of memory effects. In this context, it is very instructive to view the QENS data and our fits after Fourier transformation as intermediate scattering functions $I(Q, t)$ (Fig. 3). The stretched sample exhibits a dynamic behavior not explained using the usual Rouse and stretched-exponential approaches. Not only does the increased α indicate a considerable loss of memory by stretching, with the dynamics much closer to Markov processes than in native silk, but the decrease of the fractional relaxation time τ by almost an order of magnitude (from 95 to 10 ps) confirms a much shorter time scale of the molecular motions.

In conclusion, we have provided experimental evidence for a link between the macroscopic viscoelastic long-time relaxation and the stationary diffusion processes on the molecular scale in polymers: both are described on the basis of the same fractional relaxation processes, which strongly depend on the macroscopic stretching state.

We acknowledge funding by the Deutsche Forschungsgemeinschaft (SFB-677 Function by Switching) and stimulating discussions with I. Greving (HZG), M. Koza (ILL), and W. Press (Kiel University).

-
- [1] Z. Shao, F. Vollrath, *Nature* **418**, 741 (2002)
 - [2] J. Gosline, M. DeMont, M. Denny, *Endeavour* **10**, 37 (1986)
 - [3] C. Riekel, M. Gutierrez, A. Gourrier, S. Roth, *Analytical and Bioanalytical Chemistry* **376**, 594 (2003)
 - [4] D. Sapede, T. Seydel, V. Forsyth, M.M. Koza, R. Schweins, F. Vollrath, C. Riekel, *Macromolecules* **38**, 8447 (2005)
 - [5] Y. Shen, M. Johnson, D. Martin, *Macromolecules* **31**, 8857 (1998)
 - [6] O. Hakimi, D. Knight, M. Knight, M. Grahn, P. Vadgama, *Biomacromolecules* **7**, 2901 (2006)
 - [7] C. Holland, A. Terry, D. Porter, F. Vollrath, *Nature Mat.* **5**, 870 (2006)
 - [8] A. Glišovic, T. Vehoff, R. Davies, T. Salditt, *Macromolecules* **41**, 390 (2008)
 - [9] I. Krasnov, I. Diddens, N. Hauptmann, G. Helms, M. Ogurreck, T. Seydel, S.S. Funari, M. Müller, *Phys.Rev.Lett.* **100**, 048104 (2008)
 - [10] J. Gosline, M. Denny, M. Demont, *Nature* **309**, 551 (1984)
 - [11] T. Seydel, K. Kölln, I. Krasnov, I. Diddens, N. Hauptmann, G. Helms, M. Ogurreck, S.G. Kang, M.M. Koza, M. Müller, *Macromolecules* **40**, 1035 (2007)
 - [12] R. Bagley, P. Torvik, *Journal of Rheology* **27**, 201 (1983)
 - [13] A. Drozdov, *Acta mechanica* **124**, 155 (1997)
 - [14] W. Gloeckle, T. Nonnenmacher, *Macromolecules* **24**, 6426 (1991)
 - [15] R. Zwanzig, *Phys. Rev.* **124**, 983 (1961)
 - [16] W. Glöckle, T. Nonnenmacher, *Rheol.Acta* **33**, 337 (1994)
 - [17] R. Metzler, J. Klafter, *Physics Reports* **339**, 1 (2000)
 - [18] F. Mainardi, *Fractional calculus and waves in linear viscoelasticity: An introduction to mathematical models*

- (Imperial College Press, 2010)
- [19] Z. Jiang, W. Schoufelberger, M. Thoma, A. Wyner, *Block pulse functions and their applications in control systems* (Springer New York, 1992)
- [20] T. Seydel, W. Knoll, I. Greving, C. Dicko, M.M. Koza, I. Krasnov, M. Müller, *Phy.Rev.E* **83**, 016104 (2011)
- [21] R. Hilfer, H. Seybold, *Integral Transforms and Special Functions* **17**, 637 (2006)
- [22] P. Rouse, *J.Chem.Phys.* **21**, 1272 (1953)
- [23] N. Heymans, J.C. Bauwens, *Rheol.Acta* **33**, 210 (1994)
- [24] G. Kneller, K. Hinsén, *J.Chem.Phys.* **121**, 10278 (2004)